



# Research Progress of CXCR4-Targeting Radioligands for Oncologic Imaging

Yanzhi Wang, Feng Gao

Key Laboratory for Experimental Teratology of the Ministry of Education and Research Center for Experimental Nuclear Medicine, School of Basic Medical Sciences, Cheeloo College of Medicine, Shandong University, Jinan, Shandong, China

C-X-C motif chemokine receptor 4 (CXCR4) plays a key role in various physiological functions, such as immune processes and disease development, and can influence angiogenesis, proliferation, and distant metastasis in tumors. Recently, several radioligands, including peptides, small molecules, and nanoclusters, have been developed to target CXCR4 for diagnostic purposes, thereby providing new diagnostic strategies based on CXCR4. Herein, we focus on the recent research progress of CXCR4-targeting radioligands for tumor diagnosis. We discuss their application in the diagnosis of hematological tumors, such as lymphomas, multiple myelomas, chronic lymphocytic leukemias, and myeloproliferative tumors, as well as nonhematological tumors, including tumors of the esophagus, breast, and central nervous system. Additionally, we explored the theranostic applications of CXCR4-targeting radioligands in tumors. Targeting CXCR4 using nuclear medicine shows promise as a method for tumor diagnosis, and further research is warranted to enhance its clinical applicability.

**Keywords:** CXCR4; Radioligands; Nuclear medicine; Imaging; Neoplasm; Oncology; Cancer

## INTRODUCTION

Diagnostic techniques in nuclear medicine, including positron emission computed tomography (PET) and single photon emission computed tomography (SPECT), have demonstrated their potential and reliability in early diagnosis, staging, the detection of metastasis, and the guidance for subsequent treatments for tumors. C-X-C motif chemokine receptor 4 (CXCR4) is highly expressed in several tumors involving the breast, prostate, lung, and colorectum, and it could also promote tumor progression and metastasis. The development of diagnostic technologies in nuclear medicine based on CXCR4 has expanded considerably to

include various types of tumors. Table 1 summarizes several radiotracers that have been extensively studied clinically, and some novel radiotracers have been developed in recent years [1-21]. This review discusses progress in CXCR4 targeting radioligands for the diagnosis of various types of tumors.

## Physiological and Pathological Roles and Mechanisms of CXCR4

CXCR4 is a seven-transmembrane G protein-coupled receptor with a highly conserved structure comprising 352 amino acid residues, including one amino (N)-terminus, one carboxyl (C)-terminus, seven transmembrane helices, and three extracellular and intracellular loops [22-24]. CXCR4 is a member of the chemokine receptor family that plays an important role in numerous physiological processes and signaling pathways. Chemokine receptors mediate the function of chemokines in target cells, thereby activating protein kinases and promoting intracellular  $Ca^{2+}$  mobilization [25]. CXCR4 was first identified in peripheral blood leukocytes, and is widely expressed throughout the body during embryonic development and adulthood in a variety of cell types [23,26], including lymphocytes, endothelial

**Received:** January 31, 2023 **Revised:** May 24, 2023

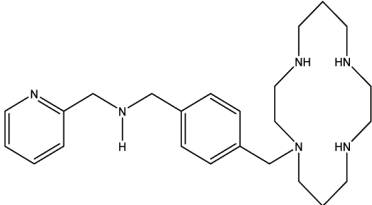
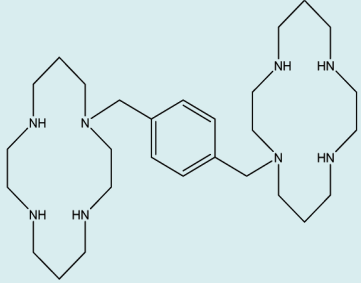
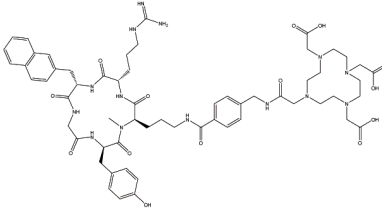
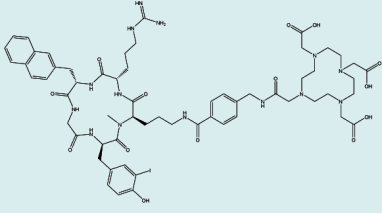
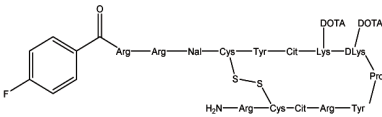
**Accepted:** July 7, 2023

**Corresponding author:** Feng Gao, PhD, Key Laboratory for Experimental Teratology of the Ministry of Education and Research Center for Experimental Nuclear Medicine, School of Basic Medical Sciences, Cheeloo College of Medicine, Shandong University, No.44 Wenhua Xi Road, Jinan, Shandong 250012, China

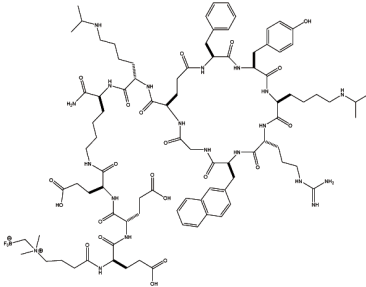
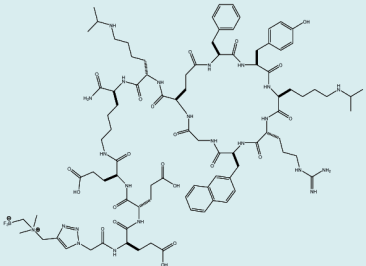
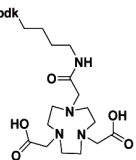
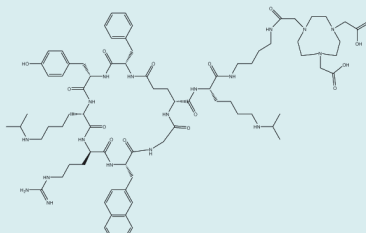
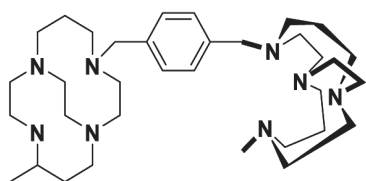
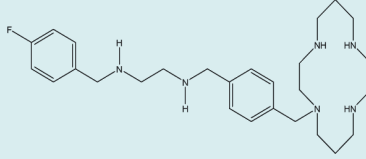
• E-mail: rrgaofeng@sdu.edu.cn

This is an Open Access article distributed under the terms of the Creative Commons Attribution Non-Commercial License (<https://creativecommons.org/licenses/by-nc/4.0>) which permits unrestricted non-commercial use, distribution, and reproduction in any medium, provided the original work is properly cited.

**Table 1.** Summary of CXCR4-targeted radiotracer

Compound	Radioactive isotope	Labeling method	Target molecular structure	Applied disease	Human research (Y/N)	Application	Ref.
AMD3465	$^{64}\text{Cu}$	$^{64}\text{Cu}$ pH = 5–5.5 55°C–60°C 45 min		Colon adenocarcinoma and glioma	N	Diagnosis	[1]
AMD3100	$^{68}\text{Ga}$ $^{64}\text{Cu}$ $^{99\text{m}}\text{Tc}$	$^{68}\text{Ga}$ pH = 4.5 90°C 15 min  $^{64}\text{Cu}$ pH = 5.5 25°C 60 min  $^{99\text{m}}\text{Tc}$ sodium [ $^{99\text{m}}\text{Tc}$ ] pertechnetate + $\text{SnCl}_2$ pH = 7.2 25°C 20 min		Lymphoma, glioma, ACC, WM	Y	Diagnosis	[2,7]
Pentixafor	$^{68}\text{Ga}$	pH = 4.5 90°C 15 min		Various cancer, cardiac diseases, infectious and autoimmune diseases	Y	Diagnosis	[8-10]
Pentixather	$^{177}\text{Lu}$ $^{64}\text{Cu}$ $^{90}\text{Y}$	$^{177}\text{Lu}$ pH = 6.0 95°C 30 min  $^{64}\text{Cu}$ pH = 5.5 25°C 60 min  $^{90}\text{Y}$ pH = 6.0 95°C 30 min		Various cancer	Y	Diagnosis and Therapy	[11-14]
T140-2D	$^{64}\text{Cu}$	pH = 5.5 40°C 20 min		Lymphoma	N	Diagnosis	[15]

**Table 1.** Summary of CXCR4-targeted radiotracer (continued)

Compound	Radioactive isotope	Labeling method	Target molecular structure	Applied disease	Human research (Y/N)	Application	Ref.
BL08	<sup>18</sup> F	pH = 2.0 80°C 20 min		Lymphoma	N	Diagnosis	[16]
BL09	<sup>18</sup> F	pH = 2.0 80°C 20 min		Lymphoma	N	Diagnosis	[16]
NOTA-DV1-k- (DV3)	<sup>18</sup> F	pH = 2.0 80°C 20 min	$\text{H}_2\text{N}-\text{Igaswhrpdkcclgyqkrpk}-\text{COOH}$ 	Lymphoma	N	Diagnosis	[17]
NOTA-CP01	<sup>64</sup> Cu	pH = 5–5.5 55°C–60°C 45 min		Esophageal cancer	N	Diagnosis	[18]
CB-bicyclam	<sup>64</sup> Cu	pH = 5–5.5 55°C–60°C 45 min		Glioblastoma astrocytoma	N	Diagnosis	[19]
MCFB	<sup>18</sup> F	pH = 2.0 80°C 20 min		Triple-negative metastatic breast Cancer, diffuse large B-cell Lymphoma	N	Diagnosis	[20]

ACC = adrenocortical carcinoma, WM = Waldenström macroglobulinemia, Y = yes, N = no

cells, epithelial cells, hematopoietic stem cells, stromal fibroblasts, and tumor cells [23,27]. In addition to its functions in hematopoietic and immune responses, CXCR4

plays a vital role in neurogenesis, germ cell development, cardiogenesis, and angiogenesis [27-34]. CXCR4 expression is closely associated with various diseases. It was originally

discovered to function as a coreceptor for T-tropic (X4) human immunodeficiency virus (HIV), which enters CD4<sup>+</sup> T cells [35]. In rheumatoid arthritis, CD4<sup>+</sup> memory T cells accumulate in the inflamed synovium and express CXCR4 [36]. CXCR4 is involved in the development of chronic inflammation of the arterial wall and mediates the influx of leukocytes [37]. Moreover, CXCR4 plays an important role in vascular remodeling, atherosclerotic plaque instability, and aneurysm formation after injury [38]. Additionally, the inflammatory process of local esophageal infiltration by CXCR4<sup>+</sup> immune cells strongly promotes esophageal carcinogenesis [39]. CXCR4 is associated with monocyte recruitment and endothelial injury in atherosclerosis [40]. In addition to participating in various inflammation-related processes, CXCR4 dysregulation contributes substantially to the occurrence of neurodegenerative diseases [41]. Furthermore, CXCR4 has a major effect on the evolution and metastasis of many tumors [42-51], and can mediate organ-specific metastasis of tumors and act as a predictor of the metastatic potential of specific tumor types [52-54]. CXCR4 also has an impact on cancer stem cells [55,56].

The combination of CXCL12 and CXCR4 activates various signaling pathways. CXCL12-CXCR4 forms a complex with the G $\alpha$ i subunit G protein, inhibits the production of cyclic adenosine monophosphate mediated by adenylate cyclase, promotes the mobilization of intracellular calcium ions [57], and activates multiple signaling pathways, including RAS-MAPK, PI3K-AKT-mTOR, JAK-STAT, Akt, JNK, MEK, and ERK1/2, thereby promoting tumor proliferation, inhibiting cancer cell apoptosis, and promoting metastasis [53]. For example, the G $\alpha$  subunit can induce FAK, ERK, and Akt signaling in pancreatic cancer cells, thus enhancing the transcriptional activity of  $\beta$ -catenin and NF- $\kappa$ B. It can also activate the Ras and Rac/Rho pathways, leading to the phosphorylation of ERK and p38 proteins. The G $\alpha$  subunit may also be involved in polarization and chemotaxis, induction of cell migration, and expression of survival proteins. Moreover, the activation of CXCL12 can induce the recruitment of the  $\beta$ -repressor to CXCR4, thus enhancing signal transduction or inducing receptor internalization. CXCR4 is uncoupled through G protein-coupled receptors kinase (GRK)-dependent phosphorylation and G proteins interacting with  $\beta$ -repressor desensitization [58]. Most G protein-coupled receptors (GPCRs) activate both the  $\beta$ -repressor and G protein signaling pathways, CXCR4- $\beta$ -repressor interaction induces receptor desensitization and endocytosis in cells in the absence of agonist stimulation.

In contrast, the  $\beta$ -repressor enhances CXCL12-induced chemotaxis and CXCL12-mediated activation of the p38-MAPK pathway [59,60]. Because of the aforementioned effects of CXCR4 in cancer, it is expected to become an important target for cancer treatment. Many drug delivery systems that target CXCR4 have been developed, including liposomes [61], nanoparticles [62], lipases [63], and polymerases [64].

## Diagnostic Applications for Hematological Tumors

Modern molecular imaging techniques have been widely applied over the past two decades for the early assessment of treatment response and early detection of tumor metastasis in hematological tumors [65-68]. Pentixafor is a cyclic pentapeptide with DOTA (1,4,7,10-Tetraazacyclododecane-1,4,7,10-tetraacetic acid) as the metal-chelating agent, and its targeting vector was designed based on the cyclic pentapeptide developed by Fujii et al. [27]. Pentixafor uptake has been observed in many malignancies (Fig. 1) [8]. In 2015, Wester et al. [65] first reported the clinical application of <sup>68</sup>Ga-Pentixafor PET as an efficient method for CXCR4 imaging to evaluate the potential of <sup>68</sup>Ga-Pentixafor PET in cancer research and therapy. This non-invasive imaging technique can quantitatively assess CXCR4 expression and further elucidate the role of CXCR4/CXCL12 in the pathogenesis and treatment of cancer, cardiovascular diseases, and autoimmune and inflammatory diseases. <sup>68</sup>Ga-Pentixafor is sensitive to CXCR4 expression levels. In lymphoma lesions, tracer uptake of both <sup>68</sup>Ga-Pentixafor and <sup>18</sup>F-fludeoxyglucose (F-FDG) was evident, whereas in biopsy-proven non-small cell lung cancer (NSCLC) lesions, <sup>68</sup>Ga-Pentixafor uptake was significantly lower than that of <sup>18</sup>F-FDG. Immunohistochemistry (IHC) confirmed CXCR4 expression in lymphoma lesions, whereas in lung biopsies, only a few infiltrating plasma cells were CXCR4-positive and tumors were CXCR4-negative. The authors argued that these two tracers could provide complementary information on tumor spread and biology. In some patients, <sup>68</sup>Ga-Pentixafor uptake was higher than that of <sup>18</sup>F-FDG. Therefore, <sup>68</sup>Ga-Pentixafor PET may be the imaging modality of choice. Moreover, some advantages of <sup>68</sup>Ga-Pentixafor are highlighted. For example, it can quantitatively provide detailed information related to CXCR4 expression in various diseases and may provide a new tool for patient stratification, treatment choice, and disease monitoring.

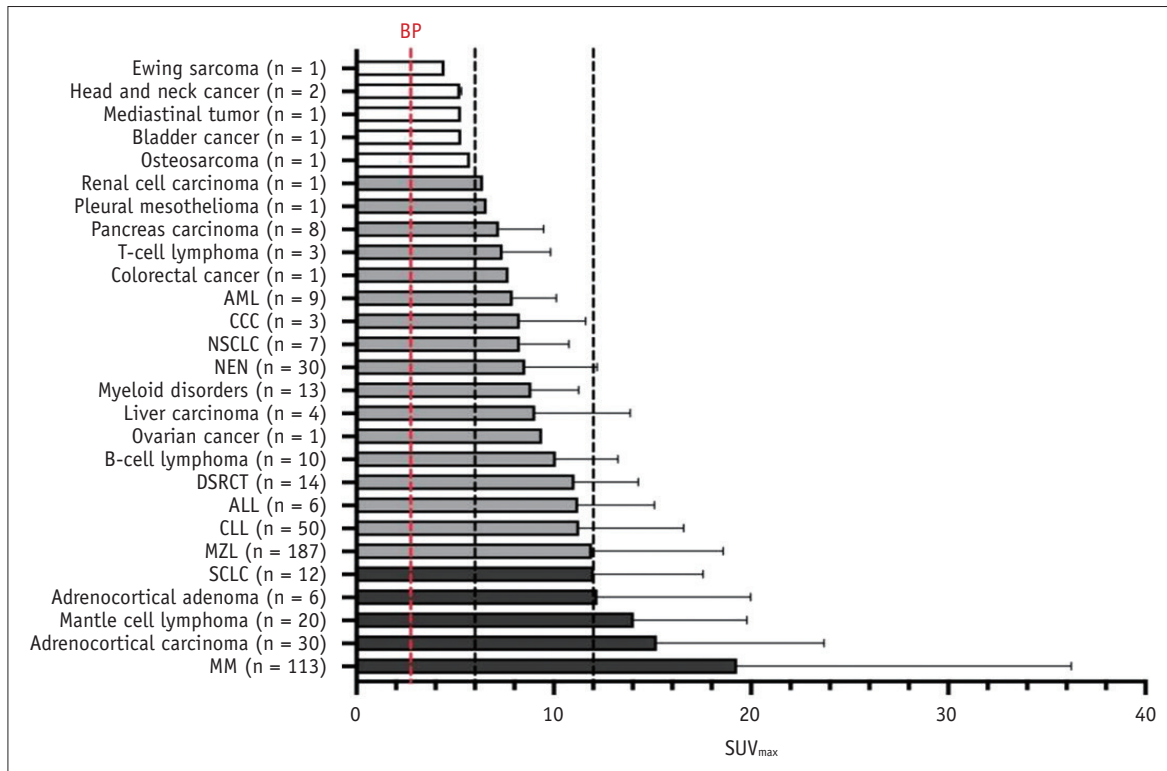


**Fig. 1.** Bar chart displaying average SUV<sub>max</sub>. Mean ± standard deviation is indicated. Black dotted lines show SUV<sub>max</sub> cutoffs of 6 and 12, respectively. In individual lesions, a markedly increased SUV<sub>max</sub> of up to 85.8 was observed. Number of investigated patients (n) per diagnosis group is given in parentheses. This research was originally published in *JNM*. Buck et al., Imaging of C-X-C motif chemokine receptor 4 expression in 690 patients with solid or hematologic neoplasms using (68)Ga-pentixafor PET, *J Nucl Med* 2022;63:1687-1692 [8]. ©SNMMI; <https://doi.org/10.2967/jnumed.121.263693>. BP = blood pool (red dotted line), AML = acute myeloid leukemia, CCC = cholangiocarcinoma, NSCLC = non-small cell lung carcinoma, NEN = neuroendocrine neoplasm, DSRCT = desmoplastic small round cell tumor, ALL = acute lymphoblastoid leukemia, CLL = chronic lymphocytic leukemia, MZL = marginal zone lymphoma, SCLC = small cell lung carcinoma, MM = multiple myeloma

<sup>68</sup>Ga-Pentixafor PET imaging has opened up a broad field of clinical research to explore the correlation between CXCR4 expression and the regulation of diverse biological processes.

### Lymphoma

The staging and localization of extranodal and marginal zone B-cell lymphomas in mucosa-associated lymphoid tissue (MALT) lymphomas represent a significant challenge for imaging. In general, CT scans of the chest, abdomen, and pelvis, in combination with physical examinations, are recommended for diagnosis, although the diagnostic accuracy of this method is not as expected [69].

In 2019, Haug et al. [70] evaluated the noninvasive detection of MALT lymphoma using <sup>68</sup>Ga-Pentixafor PET/magnetic resonance imaging (MRI). In this prospective proof-of-concept study, 36 patients with MALT lymphoma who had not previously received systemic or radiation therapy were investigated. In total, 33 patients with MALT

lymphoma showed increased <sup>68</sup>Ga-Pentixafor uptake with a favorable tumor-to-background ratio, and the remaining 3 patients underwent orbital MALT lymphoma surgery before PET/MRI (Fig. 2). <sup>68</sup>Ga-Pentixafor PET/MRI was feasible for MALT lymphoma evaluation, with a good tumor-to-background ratio of radiotracer uptake. Notably, uptake varied widely among patients, and the authors speculated that the extent of <sup>68</sup>Ga-Pentixafor uptake may be associated with prognosis. Therefore, <sup>68</sup>Ga-Pentixafor not only has ideal diagnostic accuracy but can also be used for non-invasive prognostic stratification. In addition, <sup>68</sup>Ga-Pentixafor was found in 17% of patients with lymphoma manifestations not seen on MRI, which could affect tumor staging and subsequent treatment options [70].

Mantle cell lymphoma (MCL) is one of the five most common non-Hodgkin lymphomas with a variable clinical course, most of which are rapidly invasive, and a few are slow-growing, indolent diseases. Despite the availability of novel treatments, the prognosis of patients with MCL

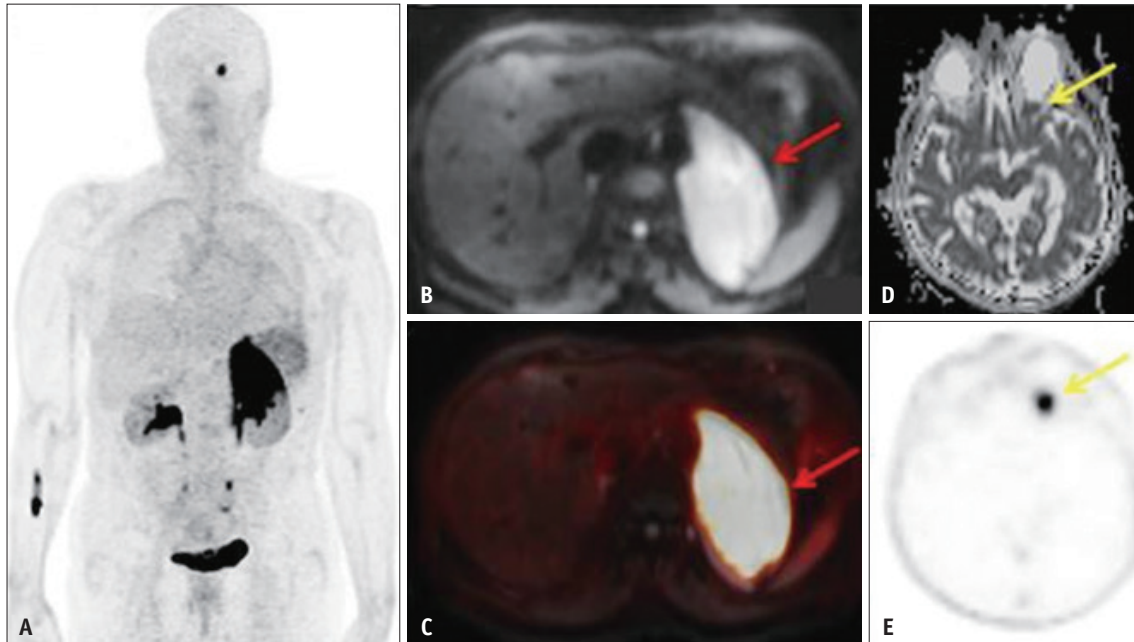


**Fig. 2.** A patient with biopsy-proven mucosa-associated lymphoid tissue (MALT) lymphoma of the left adrenal gland. The adrenal MALT lymphoma shows high  $^{68}\text{Ga}$ -Pentixafor uptake (**A**) and is also well-visualized on the diffusion-weighted imaging b800 image (red arrows in **B** and **C**, fused PET/MRI). In addition, an area of increased uptake on PET is visible in the left orbit (**E**, yellow arrow), which was initially missed on MRI, but, in retrospect, showed restricted diffusion on the apparent diffusion coefficient map upon consensus reading (**D**, yellow arrow). Reprinted from Haug et al., Prospective non-invasive evaluation of CXCR4 expression for the diagnosis of MALT lymphoma using [(68)Ga]Ga-pentixafor-PET/MRI, *Theranostics* 2019;9:3653-3658 [70].

remains poor, with a 5-year survival rate of approximately 50% [71].

In 2021, Mayerhoefer et al. [71] carried out a prospective study of patients with MCL to evaluate the effect of the CXCR4 tracer  $^{68}\text{Ga}$ -Pentixafor compared with  $^{18}\text{F}$ -FDG using PET images of MCL. This study included 22 patients with MCL. The results showed that the sensitivity of  $^{68}\text{Ga}$ -Pentixafor was significantly higher than that of  $^{18}\text{F}$ -FDG (Fig. 3). In each region, the detection rate of  $^{68}\text{Ga}$ -Pentixafor for lymphoma was significantly higher than that of  $^{18}\text{F}$ -FDG, with a sensitivity difference of +25%. Furthermore, the standard uptake value (SUV) and tumor-to background ratio (TBR) were significantly higher than those of  $^{18}\text{F}$ -FDG (2–2.5-fold), while the uptake of  $^{68}\text{Ga}$ -Pentixafor was significantly correlated with the expression of CXCR4 in MCL cells, as demonstrated by IHC. The positive predictive value (PPV) of  $^{68}\text{Ga}$ -Pentixafor decreased slightly in 6 of 22 patients but was not significant because of the increased  $^{68}\text{Ga}$  uptake in non-enlarged cervical lymph nodes. There was no difference in the staging of the individual patients. In this study, the authors determined a threshold for  $^{68}\text{Ga}$  uptake for splenic involvement in hematological malignancies for the first time. The data showed that the tumor-to-background ratio

performed well regarding assessing lymphoma involvement with a cut-off value of 4.0 and a negative predictive value of 91%, thus indicating a faint probability of malignancy below this threshold. Therefore,  $^{68}\text{Ga}$ -Pentixafor provided a higher detection rate and better tumor background contrast than  $^{18}\text{F}$ -FDG and could evaluate the involvement of the spleen, possibly representing a replacement for  $^{18}\text{F}$ -FDG in the detection of MCL [71].

Waldenström macroglobulinemia (WM), a B-cell malignancy, is a rare low-grade non-Hodgkin lymphoma characterized by the secretion of monoclonal immunoglobulin M (IgM) into the peripheral blood and lymphoplasmacytic infiltration. CXCR4 expression in WM cell lines varies, and hypoxia promotes cancer cell invasion by upregulating CXCR4 expression [72].

In 2020, a study investigated the possibility of targeting CXCR4 to detect WM cells. Muz et al. [4] used  $^{64}\text{Cu}$  to label the CXCR4 inhibitor, AMD3100, and detected its binding to WM cells with different CXCR4 expression levels. PET/CT scans were used to detect tracer accumulation in subcutaneous and intratibial models, while the differential amounts of WM cells in peripheral blood mononuclear cells were detected by gamma counting. Analysis showed



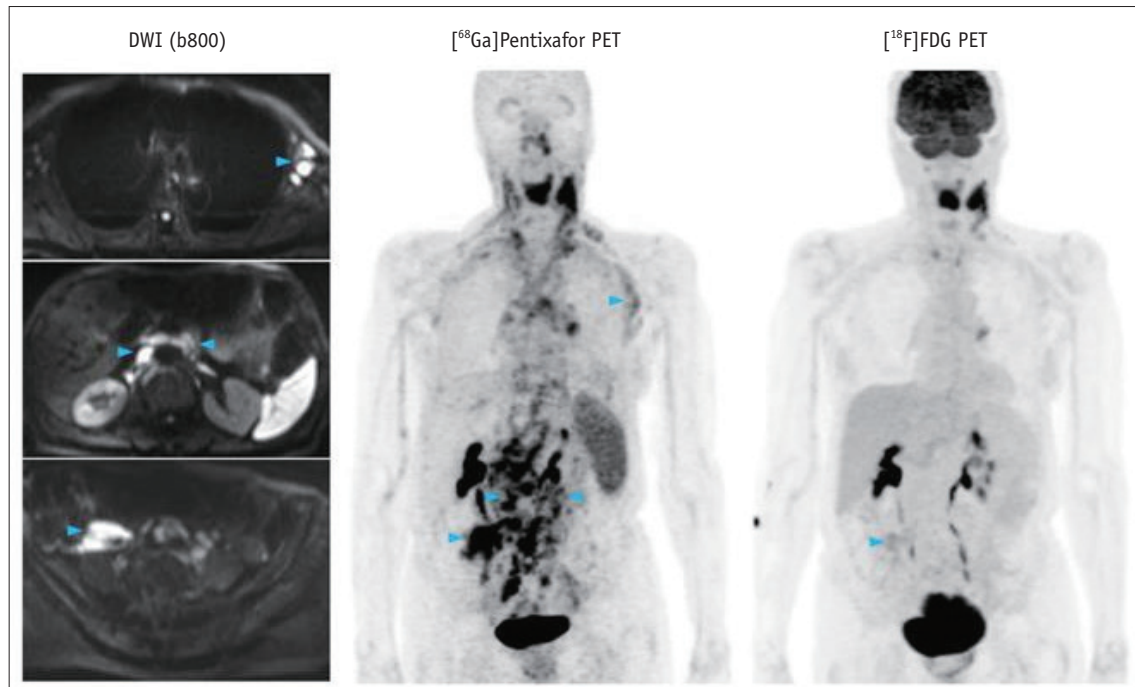


**Fig. 3.** Pre-therapeutic  $^{68}\text{Ga}$ -Pentixafor-PET/MRI and  $^{18}\text{F}$ -FDG-PET/MRI of an 82-year-old female patient with mantle cell lymphoma. Representative examples of such  $^{68}\text{Ga}$ -Pentixafor-PET-positive lesions with no or low  $^{18}\text{F}$ -FDG uptake, but obvious lymphadenopathy on diffusion-weighted imaging (DWI), are marked by blue arrowheads (left axially, retroperitoneal/periaortic, and right pelvic regions). Reprinted from Mayerhoefer et al., CXCR4 PET imaging of mantle cell lymphoma using [(68)Ga]Pentixafor: comparison with [(18)F]FDG-PET, *Theranostics* 2021;11:567-578 [71]. FDG = fludeoxyglucose

that, in vitro, the accumulation of  $^{64}\text{Cu}$ -AMD3100 was directly correlated with the CXCR4 expression levels in WM cells. Under hypoxic conditions, CXCR4 expression levels in cells increased with a corresponding increase in tracer accumulation; conversely, when CXCR4 and hypoxia inducible factor (HIF)-1 $\alpha$  were knocked down, the binding of the tracer to cells was reduced. In addition,  $^{64}\text{Cu}$ -AMD3100 can detect WM cells with high levels of CXCR4 expression in the foci and circulation. These WM cells are more likely to metastasize. These results show that  $^{64}\text{Cu}$ -AMD3100 can specifically bind to CXCR4 and detect hypoxia-induced WM cells with metastatic potential in subcutaneous and intratibial models. Thus,  $^{64}\text{Cu}$ -AMD3100 is a sensitive and promising tumor tracer and is expected to predict the possibility of WM cell spread and metastasis [4].

Marginal zone lymphoma (MZL) originates from malignantly transformed lymphocytes of the B cell lineage and belongs to the family of non-Hodgkin lymphomas. These three subtypes are distinguished based on their tissue of origin. The most common subtype is extranodal MZL, which originates from MALT and accounts for 70% of all MZL cases. Splenic MZL and lymph node MZL subtypes are less common and primarily affect the spleen or lymph nodes; however, they

can also be found in the peripheral blood or bone marrow [73].

In 2021, Duell et al. [73] explored the value of  $^{68}\text{Ga}$ -Pentixafor for the staging of marginal zone lymphomas. These authors added CXCR4-targeting  $^{68}\text{Ga}$ -Pentixafor imaging to conventional and routine staging and used  $^{68}\text{Ga}$ -Pentixafor to investigate 22 newly diagnosed patients with MZL. The staging of CXCR4 PET/CT and comparison of biopsy and imaging results of the lesions were used to determine the impact of CXCR4-targeted  $^{68}\text{Ga}$ -Pentixafor on imaging for staging and treatment options. The analysis showed that CXCR4 PET/CT correctly detected all true positive (TP) and true-negative patients, 75% of patients with gastrointestinal involvement, and all patients with bone marrow (BM) infiltration. CXCR4 PET/CT also correctly detected all MZL and true-negative cases, whereas conventional staging identified only 20 TPs. Of the 16 TPs, 1 TP patient, and 2 true-negative patients, CXCR4-targeted PET/CT detected more MZL manifestations per patient and per lesion than conventional staging. Notably, some lesions that are easily missed, such as subcutaneous or orbital masses, can be visualized using this new imaging method. These data also demonstrate the non-inferiority of CXCR4 PET/CT in detecting gastrointestinal lesions and BM infiltration at sites

that were difficult to diagnose. Furthermore, this method had a substantial impact on staging, leading to restaging in almost half of the patients, which in turn had a direct impact on patient care, with more than a third of patients having their treatment regimen modified as a result [73].

### Multiple Myeloma

Multiple myeloma (MM) is a malignant disease characterized by the neoplastic proliferation of plasma cells in the bone marrow, producing monoclonal immunoglobulins [74,75]. Although the overall survival (OS) of patients with MM has improved over the past decade, it remains largely incurable.

In 2017, Lapa et al. [76] evaluated the role of <sup>68</sup>Ga-Pentixafor in the diagnosis of multiple myeloma. A total of 35 patients with MM were included in this study for <sup>68</sup>Ga-Pentixafor PET/CT imaging, 19 of whom underwent <sup>18</sup>F-FDG imaging. Of the 35 patients imaged with <sup>68</sup>Ga-Pentixafor, 23 were CXCR4<sup>+</sup> (Fig. 4). Of the 19 patients who received both <sup>68</sup>Ga-Pentixafor and <sup>18</sup>F-FDG, 11 were positive for both tracers, and 4 were negative for both tracers. Three patients were negative only for <sup>68</sup>Ga-Pentixafor on imaging. Compared

with <sup>18</sup>F-FDG imaging, <sup>68</sup>Ga-Pentixafor detected more lesions in four patients, <sup>18</sup>F-FDG detected more lesions in seven patients, and two tracers were detected in the remaining eight patients. The number of lesions was the same; that is, <sup>68</sup>Ga-Pentixafor had a sensitivity equal to or better than <sup>18</sup>F-FDG in 63% of cases. For the detection of extramedullary disease, <sup>68</sup>Ga-Pentixafor and <sup>18</sup>F-FDG performed identically. OS and time to tumor progression (TTP) did not differ significantly between the two methods when patients were stratified according to median tracer uptake in the lesions. In this experiment, <sup>68</sup>Ga-Pentixafor positivity was not significantly associated with various laboratory parameters, including lactate dehydrogenase, albumin, creatinine,  $\beta_2$ M, M protein, free serum light chain levels, cytogenetic risk status, and myeloma type. These results showed that <sup>68</sup>Ga-Pentixafor can non-invasively detect CXCR4 expression in multiple myeloma and that CXCR4 expression is a negative prognostic factor for lesions and a potential target for treatment. However, <sup>68</sup>Ga-Pentixafor is clinically more useful for CXCR4-directed therapy and prognostic stratification than for myeloma diagnosis [76].

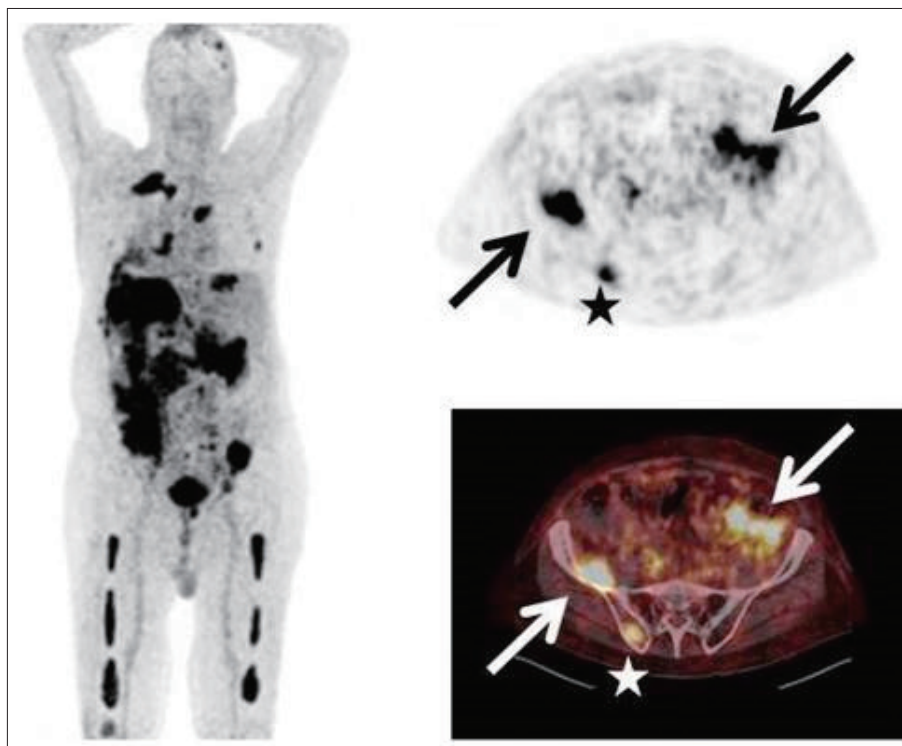


**Fig. 4.** A patient with multiple myeloma immunoglobulin A  $\lambda$  and rising free serum light chains. <sup>68</sup>Ga-Pentixafor-PET depicts intense tracer uptake in multiple intramedullary (stars) as well as extramedullary (arrows) lesions. Reprinted from Lapa et al., [(68)Ga]Pentixafor-PET/CT for imaging of chemokine receptor CXCR4 expression in multiple myeloma - comparison to [(18)F]FDG and laboratory values, *Theranostics* 2017;7:205-212 [76].



### Chronic Lymphocytic Leukemia

In 2018, Mayerhoefer et al. [77] conducted a prospective proof-of-principle study to determine whether the bone marrow uptake of  $^{68}\text{Ga}$ -Pentixafor in chronic lymphocytic leukemia (CLL) was higher than that in other tumors without bone marrow infiltration and whether this method could be used for CLL imaging. In this study, 13 patients with CLL and 20 controls (10 with pancreatic cancer and 10 with MALT lymphoma) underwent  $^{68}\text{Ga}$ -Pentixafor imaging. The authors measured tracer uptake by the pelvis, fourth lumbar vertebra, and "hottest lesions" in the bone. In addition, the authors measured the mean apparent diffusion coefficient values of the pelvis and various serum parameters, including serum white blood cell count, percentage of lymphocytes, lactate dehydrogenase,  $\beta_2$ -microglobulin, or C-reactive protein. The data showed that tracer uptake by the pelvis and L4 bone marrow differed between CLL, pancreatic cancer, and MALT lymphoma. There were no significant correlations between  $^{68}\text{Ga}$ -Pentixafor intake and pelvic apparent diffusion coefficient, white blood cell count, lymphocyte percentage, lactate dehydrogenase,  $\beta_2$ -microglobulin, and C-reactive protein. There was a significant negative correlation between the apparent diffusion coefficient (ADC) in the pelvis, white blood cell count, and lymphocyte percentage. These results showed that the bone marrow uptake value of patients with CLL was higher than that of patients with other malignant tumors without bone marrow involvement and that there was no significant correlation between the uptake of  $^{68}\text{Ga}$ -Pentixafor in the bone marrow and the ADC value. Thus, these two factors may act as mutually independent parameters for the detection and evaluation of therapeutic effects. Therefore,  $^{68}\text{Ga}$ -Pentixafor imaging using PET/MRI has potential as a multiparametric imaging modality for patients with CLL [77].

### Myeloproliferative Tumors

Myeloproliferative tumors (MPNs) are a group of rare hematopoietic stem cell disorders characterized by the abnormal proliferation of one or more myeloid lineages [78]. Diagnosis is often challenging owing to similarities in pathogenesis and symptoms. In 2022, Kraus et al. [79] used  $^{68}\text{Ga}$ -Pentixafor for PET/CT imaging to target CXCR4 and verify the feasibility of visualizing and quantifying the extent of involvement in MPNs. The team included 12 patients with MPNs (including four patients with primary myelofibrosis, six with essential thrombocythemia, and two with polycythemia vera) and five controls for  $^{68}\text{Ga}$ -Pentixafor

PET/CT examination compared with immunohistochemical staining, laboratory data, and spleen volumes. Analysis showed that the PET/CT results of the 12 patients in the experimental group were all CXCR4-positive, and a significantly higher tracer uptake was detected in the bone marrow (Fig. 5). CXCR4 targeting specificity was confirmed by immunohistochemical staining, thus demonstrating the feasibility of  $^{68}\text{Ga}$ -Pentixafor as a new PET/CT-targeted tracer and its value for visualizing and quantifying the extent of MPN accumulation. Notably, the dynamic changes in CXCR4 expression on PET/CT matched the effects in patients following treatment. The analysis initially identified that the high tracer accumulation in the spleen and BM decreased after treatment. Furthermore, data from previous studies suggest that megakaryocytes are a major driver of BM fibrosis in MPNs. These results are consistent with the findings of previous studies, with immunohistochemical data showing that CXCR4 is mainly expressed on the surfaces of megakaryocytic dysplastic cells. Therefore, the level of CXCR4 uptake can be used as a prognostic stratification factor in patients with MPN [79].

## Diagnostic Applications for Non-Hematological Tumors

### Esophageal Cancer

Most patients with esophageal cancer have late symptoms and cannot be treated surgically. These patients can only be treated with radiotherapy and chemotherapy; thus, their 5-year survival rate is less than 15% [80], which warrants new diagnostic methods. Currently, PET/CT has the highest sensitivity for diagnosing distant metastases of esophageal cancer. In primary esophageal cancer, high expression levels of CXCR4 were found to correlate with the clinicopathological features of the disease, and more than 50% of esophageal cancers express high levels of CXCR4 [81]. Wang et al. [82] confirmed that the spread and metastasis of esophageal cancer could be inhibited by blocking the CXCR4 pathway. In addition, Zhang et al. [83] suggested that miR-302b, a small non-coding RNA, can inhibit tumor growth by targeting CXCR4 and other key cancer related inflammation (CRI) pathways and inhibiting the expression of downstream cytokines.

In 2021, Linde et al. [84] evaluated and compared the roles of  $^{18}\text{F}$ -FDG and  $^{68}\text{Ga}$ -Pentixafor in staging and pre-radiotherapy planning in patients with esophageal cancer. In this retrospective analysis, the authors performed

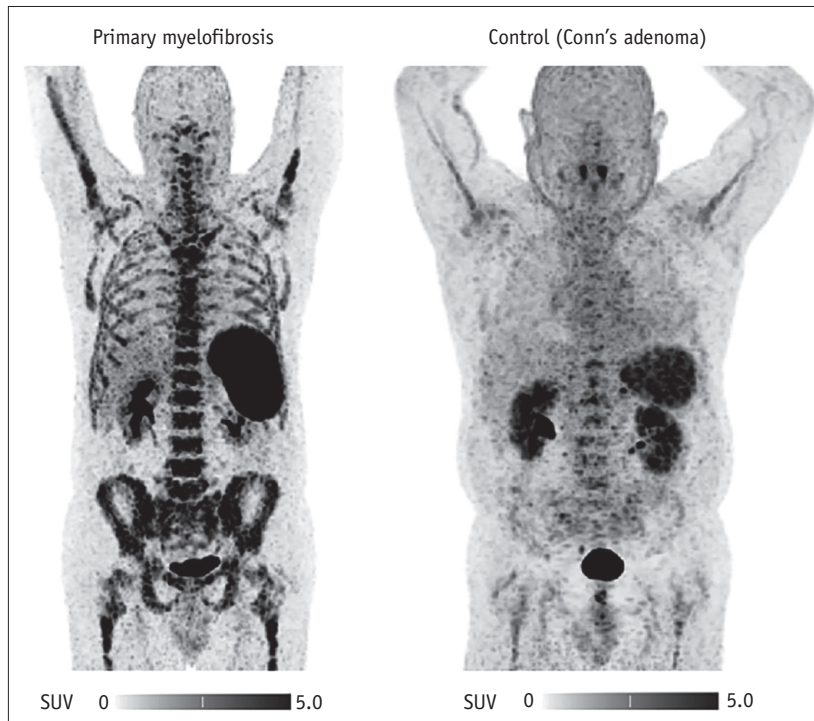


**Fig. 5.** A patient with primary myelofibrosis.  $^{68}\text{Ga}$ -pentixafor PET/CT (maximum-intensity projections) depicts significantly increased tracer uptake in the bone marrow and spleen compared with the control group. This research was originally published in *JNM*. Kraus et al., (68Ga)-pentixafor PET/CT for detection of chemokine receptor CXCR4 expression in myeloproliferative neoplasms, *J Nucl Med* 2022;63:96-99 [79]. ©SNMMI; <https://doi.org/10.2967/jnumed.121.262206>. SUV = standard uptake value

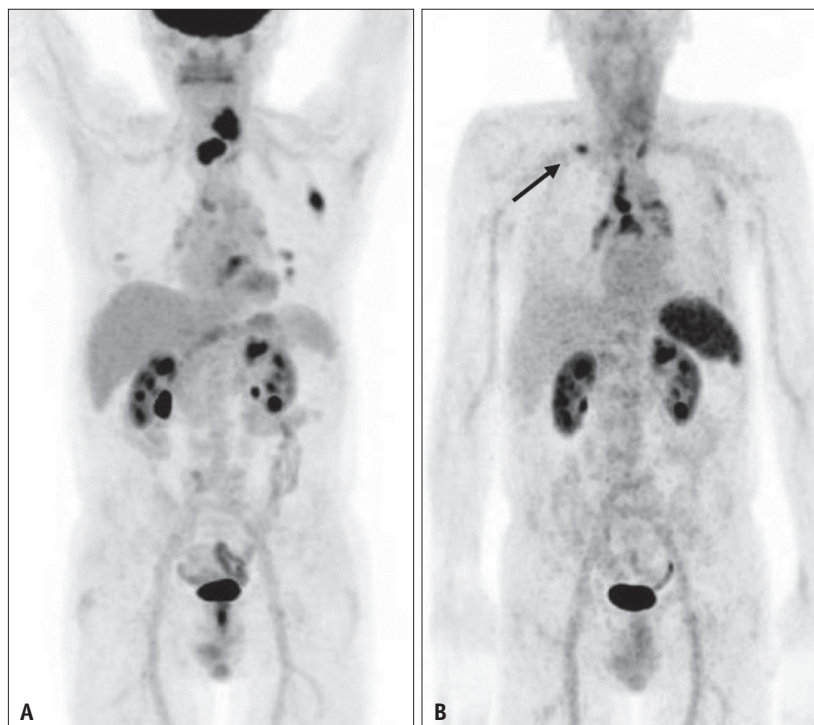


**Fig. 6.** Key lesion located peripherally to the primary tumor. Discordance of (A) FDG PET/CT and (B) non-invasive Pentixafor PET/CT imaging in one patient suffering from esophageal cancer. The lesion demonstrates high CXCR4 expression; local response was able to be shown in restaging PET/CT after radiochemotherapy. Arrow indicates the lesion. Reprinted from Linde et al., Pentixafor PET/CT for imaging of chemokine receptor 4 expression in esophageal cancer - a first clinical approach, *Cancer Imaging* 2021;21:22 [84].

Pentixafor and FDG imaging in three patients with esophageal adenocarcinoma and seven patients with esophageal squamous cell carcinoma who were scheduled to receive radiotherapy or chemotherapy (Fig. 6). The authors also performed CXCR4 immunohistochemical staining in 10 patients who underwent surgery. Analysis showed that a total of 26 lesions were detected in all patients, of which 14 were positive for both tracers, 5 were FDG<sup>+</sup> and Pentixafor<sup>-</sup>, and 7 were FDG<sup>-</sup>, but Pentixafor<sup>+</sup>. The mean uptake intensity of FDG in the lesions was slightly higher than that of Pentixafor, although the difference was not statistically significant. The physiological uptake of FDG was higher in the brain and liver, whereas Pentixafor had a higher affinity for the spleen. Imaging results were comparable to those of CXCR4 immunohistochemical staining in 7 of the 10 patients who underwent immunohistochemical staining. Of the seven patients, one was negative, two were low, two were moderate, and two were high. These results showed that PET/CT imaging of CXCR4 using Pentixafor is feasible, although there was heterogeneity among patients with different esophageal cancer. Therefore, this method can be used as a supplementary method for the diagnosis of CT, endoscopic ultrasonography (EUS), and <sup>18</sup>F-FDG in the staging and treatment of esophageal cancer [84].

### Breast Cancer

Breast cancer is the most common malignant tumor in women. Early detection, together with appropriate and effective treatment, plays a key role in improving the survival rate and prolonging the lifespan of patients. Breast-specific MRI and <sup>18</sup>F-FDG PET/CT exhibit high accuracy in the detection of breast cancer [85,86] and metastasis [87], respectively. However, with the development of personalized medicine, there is an increasing need for highly specific diagnostic and targeted therapies for breast cancer using appropriate molecular targets.

In breast cancer, CXCR4 expression and activation of its endogenous ligand, CXCL12, are key factors in tumor growth, progression, invasion, and metastasis [88-91]. CXCR4 is expressed not only by cancer cells but also by tumor-infiltrating immune cells. In the tumor microenvironment, B lymphocytes and plasmacytoid dendritic cells express CXCR4, both of which may play a role in tumor progression [57,92,93].

In 2016, Fu et al. [94] evaluated CXCR4 expression in vivo using <sup>99m</sup>Tc-labeled small interfering RNA (siRNA) as a prognostic indicator to guide the development

of personalized treatment plans and post-treatment monitoring. The authors radiolabeled CXCR4 siRNA using the bifunctional chelator hydrazine nitramide, determined the labeling efficiency, specific activity, radiochemical purity, and stability in serum, and performed biodistribution studies and static imaging in tumor-bearing mice. These data showed that the radiochemical purity of the probe remained highly stable in both fresh human serum and phosphate buffered saline, and that tumors were visible within 1–10 h after probe injection. These results indicate that <sup>99m</sup>Tc-labeled CXCR4 siRNA can be specifically aggregated and imaged in breast cancer, and may serve as a promising method to demonstrate CXCR4 expression in breast cancer [94].

In 2016, Zhao et al. [95] used <sup>64</sup>CuAuNCs-AMD3100 to target CXCR4 for the early diagnosis of breast cancer and metastasis. Nanoclusters, an emerging class of nanomaterials, have considerable potential for applications in biomedicine because of their unique size and related properties. The <sup>64</sup>CuAuNCs-AMD3100 technique not only has the targeting properties of AMD3100 but also has a significant clearance rate and low non-specific tumor retention (Fig. 7). Pharmacokinetic studies showed that <sup>64</sup>CuAuNCs-AMD3100 were well distributed in various organs within 48 h after injection and exhibited significant renal and fecal clearance. While <sup>64</sup>CuAuNCs-AMD3100 PET imaging showed that <sup>64</sup>CuAuNCs-AMD3100 had good sensitivity and accuracy in detecting CXCR4 expression at different levels, there was a strong correlation between tracer uptake and CXCR4 expression levels. Additionally, the tracer was blocked by competitive receptors, confirming its targeted specificity for CXCR4. Subsequently, the authors compared <sup>64</sup>CuAuNCs-AMD3100 with <sup>64</sup>Cu-AMD3100 and non-targeted <sup>64</sup>CuAuNCs using imaging analysis. The analysis showed that <sup>64</sup>CuAuNCs-AMD3100 was more sensitive for diagnosing early lesions and tumor metastasis while also exhibiting a lower non-specific uptake rate. Notably, as tumors progress, they undergo extensive necrosis. This may limit the delivery of CXCR4-targeted nanoclusters; however, due to receptor degradation, necrosis can also lead to reduced CXCR4 expression levels on the surface of tumor cells, thereby affecting their imaging capabilities, thus making this tool more suitable for the early evaluation of tumors. These results suggest that <sup>64</sup>CuAuNCs-AMD3100 has the potential to diagnose early-stage tumors and metastases and may contribute to the subsequent development of targeted therapy through CXCR4 or guide treatment planning in

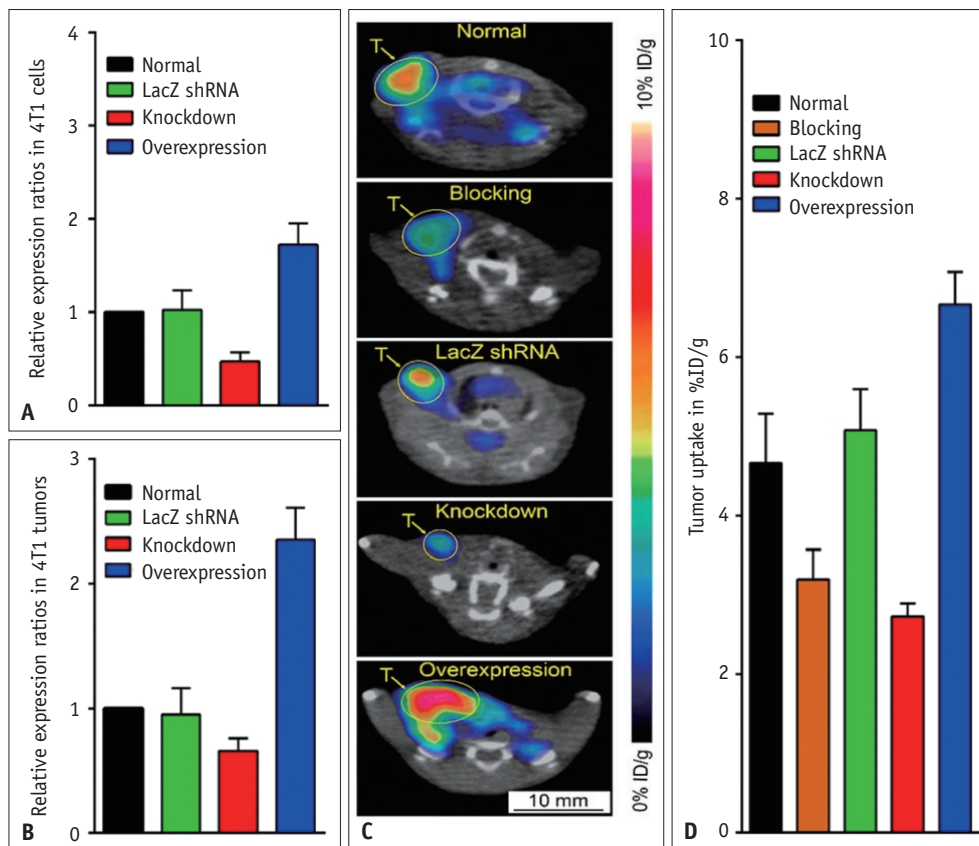


**Fig. 7.** Characterization of  $^{64}\text{Cu}$ -AuNCs-AMD3100 imaging sensitivity in engineered 4T1 models expressing various levels of CXCR4. **A:** RT-PCR of CXCR4 in normal, LacZ shRNA, knockdown, and overexpression 4T1 cells showing the different expression of receptor. **B:** RT-PCR of CXCR4 in engineered 4T1 tumors collected at 1 week post implant showing the variation of receptor levels in vivo, consistent with in vitro cell data. **C:** Representative transverse PET images demonstrating the specific detection of tumors in the engineered 4T1 tumors models. **D:** Quantitative tumor uptake of  $^{64}\text{Cu}$ -AuNCs-AMD3100 in 4T1 models showing the sensitivity detecting various CXCR4 levels. CT scale bar on representative PET/CT image was the same for all images. Reprinted with permission from Zhao et al., Gold nanoclusters doped with ( $^{64}\text{Cu}$ ) for CXCR4 positron emission tomography imaging of breast cancer and metastasis, *ACS Nano* 2016;10:5959-5970 [95]; Copyright (2016) American Chemical Society. T = tumor, RT-PCR = reverse transcription-polymerase chain reaction

breast cancer [95].

In 2019, Li et al. [96] investigated the preparation and evaluation of  $^{64}\text{Cu}$  radiolabeled ubiquitin for CXCR4 imaging. Recently, ubiquitin was identified as a natural CXCR4 ligand, offering great potential for PET imaging of CXCR4 expression. The data showed that the tumor-specific uptake of  $^{64}\text{Cu}$ -UbCG4 was significantly higher in CXCR4<sup>+</sup> 4T1 breast cancer cells than in CXCR4-knockout cells in in vitro studies. In-vivo assessments of the 4T1 xenograft mouse model showed that the tumor uptake of  $^{64}\text{Cu}$ -UbCG4 was similar to that of  $^{64}\text{Cu}$ -labeled AMD3465 but with a significantly lower background. These results suggest that  $^{64}\text{Cu}$ -UbCG4 may be an effective PET tracer for breast cancer [96].

### Tumors of the Central Nervous System

Glioblastoma is the most common primary malignant

brain tumor in adults. Conventional MRI is the preferred modality for brain tumor diagnosis because of its high soft tissue contrast and tumor sensitivity. However, conventional MRI sequences lack tumor-cell specificity. PET is similar to metabolic MRI in that it targets the molecular signatures of human tissues. Over the last few decades, some PET radioactive tracers have shown potential for brain tumor imaging, although these are still limited due to their relatively low specific uptake by tumor cells [97-100].

In 2014, Hartimath et al. [101] developed N- $^{11}\text{C}$  methyl AMD3465 as a novel CXCR4 radiotracer and tested it on rat C6 glioma and human PC-3 cell lines. These data showed that the in vitro cellular uptake of N- $^{11}\text{C}$  methyl-AMD3465 was mediated by CXCR4, and in C6 cells, transition metal ions ( $\text{Cu}^{2+}$ ,  $\text{Ni}^{2+}$  and  $\text{Zn}^{2+}$ ) enhanced the ability of this compound to bind to the cells. In contrast, ex-vivo



biodistribution and PET imaging of N-[<sup>11</sup>C]methyl-AMD3465 in C6 tumor xenografts showed that the tracer accumulated in the tumors, and tumor uptake was significantly reduced after Plerixafor (AMD3100) pretreatment, thus demonstrating that tumor uptake was CXCR4-specific. These results indicated that N-[<sup>11</sup>C]methyl-AMD3465 could detect CXCR4 expression in tumors, suggesting that N-[<sup>11</sup>C]methyl-AMD3465 may be a promising PET tracer for targeting CXCR4 [101].

Existing radiotracers are limited in targeting CXCR4 expression in central nervous system (CNS) tumors because of the blood-brain barrier (BBB) and intracellular expression of CXCR4 in tumors. In 2020, Zhang et al. [102] designed six radiotracers for imaging tumors in the central nervous system. These authors synthesized six iodinated or brominated cyclodextrin derivatives with a high affinity for CXCR4 to enhance lipophilicity and address the BBB and tumor cell membranes. The authors selected a compound with a higher specific uptake in subcutaneous tumors for further investigation in an intracranial tumor model. However, imaging CXCR4 expression in intracranial tumor models using this compound after intravenous or cerebrospinal fluid injection was not successful. The authors speculated that this was due to the hydrophilicity of the radiotracer and the existence of the BBB and tumor cell membrane barriers; thus, further investigation is necessary [102].

In 2022, Jacobs et al. [103] evaluated the diagnostic value of <sup>68</sup>Ga-Pentixafor in glioblastoma. The authors used the R2 genomics platform to detect CXCR4 mRNA expression and included seven patients with recurrent glioblastoma for <sup>68</sup>Ga-Pentixafor PET imaging and concurrent CXCR4 staining of residual resected tissue pairs. The authors identified large differences in CXCR4 expression between and within glioblastoma tumors, as well as in resected tissue from seven glioblastoma patients (Fig. 8). PET imaging results showed that the tumors from all patients showed low-to-moderate uptake, but because of the very low background activity, there was a relatively high TBR, and the CXCR4 expression levels in different patients were not completely consistent with the uptake of <sup>68</sup>Ga-Pentixafor by tumors. Therefore, the authors considered that caution should be exercised when directly converting high CXCR4 expression in isolated tissues to the high uptake of PET radiotracers; however, when <sup>68</sup>Ga-Pentixafor shows high levels of CXCR4 expression, these patients may become good <sup>177</sup>Lu-Pentixather targets for targeted radionuclide therapy [103].

Central nervous system lymphoma (CNSL) is a rare malignancy that includes primary and secondary forms.

Primary CNSL accounts for 2%–4% of all primary brain tumors and refers to a large and diffuse B-cell lymphoma confined to the central nervous system [104–106]. Secondary CNSL often presents with CNS involvement surrounding systemic lymphoma or CNS recurrence. In addition, systemic diffuse large B-cell lymphomas can also involve the central nervous system and become secondary lymphomas in the central nervous system [107–112].

Currently, contrast-enhanced brain MRI is often used to diagnose central nervous system lymphomas. Although diffusion-weighted imaging helps distinguish CNSL from other brain tumors, such as glioblastoma, its specificity has yet to be improved [113]. Furthermore, MRI is relatively inaccurate in determining complete remission [114]. However, the use of <sup>18</sup>F-FDG as a radiotracer is limited because of the physiologically high glucose uptake by healthy brain parenchyma [115]. Currently, the diagnosis must be confirmed by histopathology, especially stereotactic biopsy, which may pose challenges to the diagnosis of CNSL due to tumors located in difficult-to-biopsy locations. Therefore, the development of new targeted imaging modalities is necessary to facilitate the diagnosis of CNSL [107,116].

In 2021, Starzer et al. [117] prospectively evaluated the value of <sup>68</sup>Ga-Pentixafor in the diagnosis of central nervous system lymphoma lesions. This study included seven patients with CNSL, and <sup>68</sup>Ga-Pentixafor PET/MRI was performed for each patient. Analysis showed that <sup>68</sup>Ga-Pentixafor revealed a total of 18 lesions. In addition, all cases were confirmed by CE-MRI without false-positive lesions. Therefore, the authors believed that <sup>68</sup>Ga-Pentixafor is promising for the diagnosis of CNSL, but further research is needed to test its clinical value, such as differentiating between CNSL and glioma or between radiation-induced inflammation and residual viable tumors [117].

Vestibular schwannoma (VS) is a benign Schwann cell tumor that originates from the vestibulocochlear nerve [118]. In recent years, sporadic and neurofibromatosis-related VS have been found to significantly overexpress CXCR4. In 2019, Breun et al. [119] investigated the feasibility of <sup>68</sup>Ga-Pentixafor as a radiotracer for VS diagnosis. A total of four patients (including one newly diagnosed VS patient and three previously diagnosed or treated VS patients) were included in this study. These patients underwent <sup>68</sup>Ga-Pentixafor PET scans, and the tumors were immunohistochemically stained for CXCR4 expression. Analysis showed that the tumor lesions of



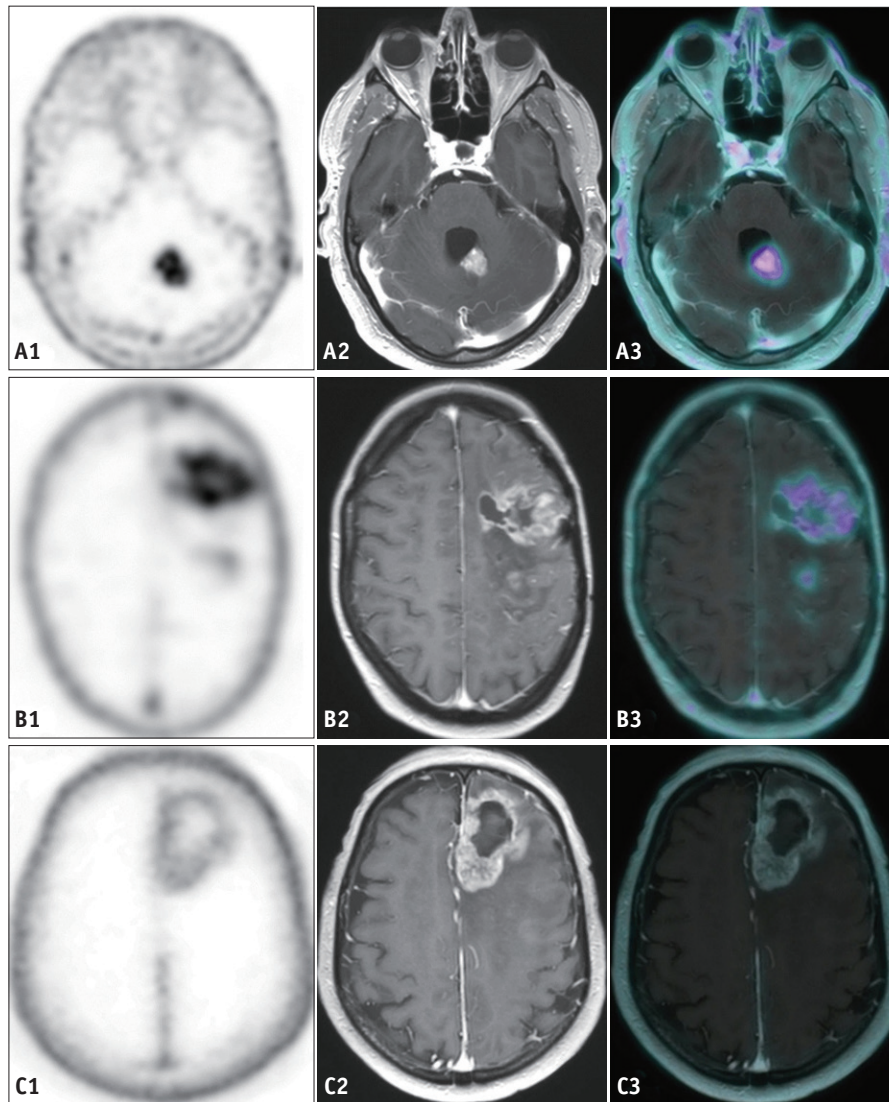


**Fig. 8.** Axial  $^{68}\text{Ga}$ -Pentixafor PET (**A1**, **B1**, **C1**), T2-weighted MRI (**A2**, **B2**, **C2**) and fused  $^{68}\text{Ga}$ -Pentixafor PET/MRI (**A3**, **B3**, **C3**) images of three patients with suspicion of recurrent glioblastoma. **A:** Male patient showing higher uptake ( $\text{SUV}_{\text{max}}$  3.5) in the MR-enhancing tissue in the left cerebellar hemisphere compared to blood-pool activity ( $\text{SUV}_{\text{mean}}$  1.48). **B:** Female patient showing low to moderate uptake ( $\text{SUV}_{\text{max}}$  1.82) in the MR-enhancing tissue in the left frontal lobe slightly higher than blood-pool activity ( $\text{SUV}_{\text{mean}}$  1.23). **C:** Male patient showing low uptake ( $\text{SUV}_{\text{max}}$  1.46) in the MR-enhancing tissue in the left frontal lobe equal to blood-pool activity ( $\text{SUV}_{\text{mean}}$  1.48). Reprinted from Jacobs et al., CXCR4 expression in glioblastoma tissue and the potential for PET imaging and treatment with [(68 Ga)Ga-pentixafor /[(177 Lu]Lu-pentixather, *Eur J Nucl Med Mol Imaging* 2022;49:481-491 [103].

all patients were positive for  $^{68}\text{Ga}$ -Pentixafor and IHC confirmed the expression of CXCR4 in VS. Therefore, the authors believe that noninvasive imaging of VS using  $^{68}\text{Ga}$ -Pentixafor PET/CT is feasible and can be used to evaluate CXCR4 expression in vivo [119].

### Theranostic Applications for Tumors

Owing to the high expression of CXCR4 in tumor tissues and its role in tumor occurrence and development, CXCR4

can not only be used for tumor monitoring, but also as a target for tumor-targeted radiotherapy. The most common theranostic methods involve the use of Ga-68 and Lu-177/Y-90 as paired nuclides. Ga-68 was used for tumor imaging, whereas Lu-177/Y-90 was used for tumor treatment. For example, Lapa et al. applied  $^{177}\text{Lu}/^{90}\text{Y}$ -pentixather for multiple myeloma treatment and used  $^{68}\text{Ga}$ -pentixafor to monitor treatment efficacy [14,120]. The imaging results showed that the treatment efficacy of  $^{177}\text{Lu}/^{90}\text{Y}$ -pentixather against CXCR4 positive tumors was obvious, with decreased

$^{68}\text{Ga}$ -pentixafor uptake in the tumor as the treatment progressed. Therefore, the theranostic application of  $^{177}\text{Lu}/^{90}\text{Y}$ -pentixather and  $^{68}\text{Ga}$ -pentixafor for CXCR4-positive tumors is of great interest and has high clinical value.

## Outlook

In recent years, understanding of the CXCR4 signaling pathway and its role in tumor progression and metastasis has improved. These developments have led to the design of CXCR4-targeting radiotracers that play an important role in tumor diagnosis, and numerous ligand structures have been developed to improve their properties. However, this system faces several challenges. For example, in central nervous system astrocytomas, the imaging effect of this tracer is affected by the BBB. Furthermore, the intracellular expression of CXCR4 can affect diagnostic accuracy [102]. Further research is required in this area. In conclusion, nuclear medicine targeting CXCR4 is a promising method for tumor diagnosis and warrants further research to improve its clinical applicability.

## Conflicts of Interest

The authors have no potential conflicts of interest to disclose.

## Author Contributions

Funding acquisition: Feng Gao. Project administration: Feng Gao. Supervision: Feng Gao. Writing—original draft: Yanzhi Wang. Writing—review & editing: Feng Gao.

## ORCID IDs

Yanzhi Wang

<https://orcid.org/0000-0003-2395-5048>

Feng Gao

<https://orcid.org/0000-0002-8792-6257>

## Funding Statement

This research was funded by grants from the Natural Science Foundation of Shandong Province (ZR2019BA015).

## Acknowledgments

This work gained great support by core facilities sharing platform of Shandong University.

## REFERENCES

1. De Silva RA, Peyre K, Pullambhatla M, Fox JJ, Pomper MG,

- Nimmagadda S. Imaging CXCR4 expression in human cancer xenografts: evaluation of monocyclam ( $^{64}\text{Cu}$ )-AMD3465. *J Nucl Med* 2011;52:986-993
2. Weiss ID, Jacobson O, Kiesewetter DO, Jacobus JP, Szajek LP, Chen X, et al. Positron emission tomography imaging of tumors expressing the human chemokine receptor CXCR4 in mice with the use of  $^{64}\text{Cu}$ -AMD3100. *Mol Imaging Biol* 2012;14:106-114
3. Renard I, Domarkas J, Poty S, Burke BP, Roberts DP, Goze C, et al. In vivo validation of ( $^{68}\text{Ga}$ )-labeled AMD3100 conjugates for PET imaging of CXCR4. *Nucl Med Biol* 2023;120-121:108335
4. Muz B, Bandara N, Mpoy C, Sun J, Alhallak K, Azab F, et al. CXCR4-targeted PET imaging using ( $^{64}\text{Cu}$ )-AMD3100 for detection of Waldenström Macroglobulinemia. *Cancer Biol Ther* 2020;21:52-60
5. Weiss ID, Huff LM, Evbuomwan MO, Xu X, Dang HD, Velez DS, et al. Screening of cancer tissue arrays identifies CXCR4 on adrenocortical carcinoma: correlates with expression and quantification on metastases using ( $^{64}\text{Cu}$ )-plerixafor PET. *Oncotarget* 2017;8:73387-73406
6. Hartimath SV, Domanska UM, Walenkamp AM, Rudi A J O D, de Vries EF. [ $^{99\text{m}}\text{Tc}$ ]O(2)-AMD3100 as a SPECT tracer for CXCR4 receptor imaging. *Nucl Med Biol* 2013;40:507-517
7. Jacobson O, Weiss ID, Szajek L, Farber JM, Kiesewetter DO. ( $^{64}\text{Cu}$ )-AMD3100--a novel imaging agent for targeting chemokine receptor CXCR4. *Bioorg Med Chem* 2009;17:1486-1493
8. Buck AK, Haug A, Dreher N, Lambertini A, Higuchi T, Lapa C et al. Imaging of C-X-C motif chemokine receptor 4 expression in 690 patients with solid or hematologic neoplasms using ( $^{68}\text{Ga}$ )-pentixafor PET. *J Nucl Med* 2022;63:1687-1692
9. Demmer O, Gourni E, Schumacher U, Kessler H, Wester HJ. PET imaging of CXCR4 receptors in cancer by a new optimized ligand. *ChemMedChem* 2011;10:1789-1791
10. Gourni E, Demmer O, Schottelius M, D'Alessandria C, Schulz S, Dijkgraaf I, et al. PET of CXCR4 expression by a ( $^{68}\text{Ga}$ )-labeled highly specific targeted contrast agent. *J Nucl Med* 2011;52:1803-1810
11. Poschenrieder A, Schottelius M, Osl T, Schwaiger M, Wester HJ. [ $^{64}\text{Cu}$ ]NOTA-pentixather enables high resolution PET imaging of CXCR4 expression in a preclinical lymphoma model. *EJNMMI Radiopharm Chem* 2017;2:2
12. Schottelius M, Osl T, Poschenrieder A, Hoffmann F, Beykan S, Hänscheid H, et al. [ $^{177}\text{Lu}$ ]pentixather: comprehensive preclinical characterization of a first CXCR4-directed endoradiotherapeutic agent. *Theranostics* 2017;7:2350-2362
13. Chen Z, Xue Q, Yao S. Nuclear medicine application of pentixafor/pentixather targeting CXCR4 for imaging and therapy in related disease. *Mini Rev Med Chem* 2023;23:787-803
14. Herrmann K, Schottelius M, Lapa C, Osl T, Poschenrieder A, Hänscheid H, et al. First-in-human experience of CXCR4-directed endoradiotherapy with ( $^{177}\text{Lu}$ - and ( $^{90}\text{Y}$ )-labeled pentixather in advanced-stage multiple myeloma with extensive intra- and extramedullary disease. *J Nucl Med*

- 2016;57:248-251
15. Jacobson O, Weiss ID, Szajek LP, Niu G, Ma Y, Kiesewetter DO, et al. PET imaging of CXCR4 using copper-64 labeled peptide antagonist. *Theranostics* 2011;1:251-262
  16. Kwon D, Lozada J, Zhang Z, Zeisler J, Poon R, Zhang C, et al. High-contrast CXCR4-targeted (18)F-PET imaging using a potent and selective antagonist. *Mol Pharm* 2021;18:187-197
  17. Luyten K, Van Loy T, Cawthorne C, Deroose CM, Schols D, Bormans G, et al. D-peptide-based probe for CXCR4-targeted molecular imaging and radionuclide therapy. *Pharmaceutics* 2021;13:1619
  18. Peng T, Wang X, Li Z, Bi L, Gao J, Yang M, et al. Preclinical evaluation of [(64)Cu]NOTA-CP01 as a PET imaging agent for metastatic esophageal squamous cell carcinoma. *Mol Pharm* 2021;18:3638-3648
  19. Burke BP, Miranda CS, Lee RE, Renard I, Nigam S, Clemente GS, et al. (64)Cu PET imaging of the CXCR4 chemokine receptor using a cross-bridged cyclam bis-tetraazamacrocyclic antagonist. *J Nucl Med* 2020;61:123-128
  20. Brickute D, Braga M, Kaliszczak MA, Barnes C, Lau D, Carroll L, et al. Development and evaluation of an (18)F-Radiolabeled monocyclam derivative for imaging CXCR4 expression. *Mol Pharm* 2019;16:2106-2117
  21. Suzuki K, Ui T, Nagano A, Hino A, Arano Y. C-terminal-modified LY2510924: a versatile scaffold for targeting C-X-C chemokine receptor type 4. *Sci Rep* 2019;9:15284
  22. Wu B, Chien EY, Mol CD, Fenalti G, Liu W, Katritch V, et al. Structures of the CXCR4 chemokine GPCR with small-molecule and cyclic peptide antagonists. *Science* 2010;330:1066-1071
  23. Lira SA, Furtado GC. The biology of chemokines and their receptors. *Immunol Res* 2012;54:111-120
  24. Loetscher M, Geiser T, O'Reilly T, Zwahlen R, Baggiolini M, Moser B. Cloning of a human seven-transmembrane domain receptor, LESTR, that is highly expressed in leukocytes. *J Biol Chem* 1994;269:232-237
  25. Hughes CE, Nibbs R. A guide to chemokines and their receptors. *FEBS J* 2018;285:2944-2971
  26. Juarez J, Bendall L, Bradstock K. Chemokines and their receptors as therapeutic targets: the role of the SDF-1/CXCR4 axis. *Curr Pharm Des* 2004;10:1245-1259
  27. Shim H, Oishi S, Fujii N. Chemokine receptor CXCR4 as a therapeutic target for neuroectodermal tumors. *Semin Cancer Biol* 2009;19:123-134
  28. Zou YR, Kottmann AH, Kuroda M, Taniuchi I, Littman DR. Function of the chemokine receptor CXCR4 in haematopoiesis and in cerebellar development. *Nature* 1998;393:595-599
  29. Moser B, Loetscher P. Lymphocyte traffic control by chemokines. *Nat Immunol* 2001;2:123-128
  30. Murphy PM. The molecular biology of leukocyte chemoattractant receptors. *Annu Rev Immunol* 1994;12:593-633
  31. Cui L, Qu H, Xiao T, Zhao M, Jolkkonen J, Zhao C. Stromal cell-derived factor-1 and its receptor CXCR4 in adult neurogenesis after cerebral ischemia. *Restor Neurol Neurosci* 2013;31:239-251
  32. Richardson BE, Lehmann R. Mechanisms guiding primordial germ cell migration: strategies from different organisms. *Nat Rev Mol Cell Biol* 2010;11:37-49
  33. Agarwal U, Ghalayini W, Dong F, Weber K, Zou YR, Rabbany SY, et al. Role of cardiac myocyte CXCR4 expression in development and left ventricular remodeling after acute myocardial infarction. *Circ Res* 2010;107:667-676
  34. Sainz J, Sata M. CXCR4, a key modulator of vascular progenitor cells. *Arterioscler Thromb Vasc Biol* 2007;27:263-265
  35. Feng Y, Broder CC, Kennedy PE, Berger EA. HIV-1 entry cofactor: functional cDNA cloning of a seven-transmembrane, G protein-coupled receptor. *Science* 1996;272:872-877
  36. Nagafuchi Y, Shoda H, Sumitomo S, Nakachi S, Kato R, Tsuchida Y, et al. Immunophenotyping of rheumatoid arthritis reveals a linkage between HLA-DRB1 genotype, CXCR4 expression on memory CD4(+) T cells, and disease activity. *Sci Rep* 2016;6:29338
  37. Galkina E, Ley K. Immune and inflammatory mechanisms of atherosclerosis (\*). *Annu Rev Immunol* 2009;27:165-197
  38. Schober A, Bernhagen J, Weber C. Chemokine-like functions of MIF in atherosclerosis. *J Mol Med (Berl)* 2008;86:761-770
  39. Fang HY, Münch NS, Schottelius M, Ingermann J, Liu H, Schauer M, et al. CXCR4 is a potential target for diagnostic PET/CT imaging in barrett's dysplasia and esophageal adenocarcinoma. *Clin Cancer Res* 2018;24:1048-1061
  40. Baba O, Huang LH, Elvington A, Szpakowska M, Sultan D, Heo GS, et al. CXCR4-binding positron emission tomography tracers link monocyte recruitment and endothelial injury in murine atherosclerosis. *Arterioscler Thromb Vasc Biol* 2021;41:822-836
  41. Bonham LW, Karch CM, Fan CC, Tan C, Geier EG, Wang Y, et al. CXCR4 involvement in neurodegenerative diseases. *Transl Psychiatry* 2018;8:73
  42. Domanska UM, Kruijzinga RC, Nagengast WB, Timmer-Bosscha H, Huls G, de Vries EG, et al. A review on CXCR4/CXCL12 axis in oncology: no place to hide. *Eur J Cancer* 2013;49:219-230
  43. Burger JA, Kipps TJ. CXCR4: a key receptor in the crosstalk between tumor cells and their microenvironment. *Blood* 2006;107:1761-1767
  44. Williams SA, Harata-Lee Y, Comerford I, Anderson RL, Smyth MJ, McColl SR. Multiple functions of CXCL12 in a syngeneic model of breast cancer. *Mol Cancer* 2010;9:250
  45. Arya M, Patel HR, McGurk C, Tatoud R, Klocker H, Masters J, et al. The importance of the CXCL12-CXCR4 chemokine ligand-receptor interaction in prostate cancer metastasis. *J Exp Ther Oncol* 2004;4:291-303
  46. Darash-Yahana M, Pikarsky E, Abramovitch R, Zeira E, Pal B, Karplus R, et al. Role of high expression levels of CXCR4 in tumor growth, vascularization, and metastasis. *FASEB J* 2004;18:1240-1242
  47. Su L, Zhang J, Xu H, Wang Y, Chu Y, Liu R, et al. Differential expression of CXCR4 is associated with the metastatic potential of human non-small cell lung cancer cells. *Clin Cancer Res* 2005;11:8273-8280



48. Phillips RJ, Burdick MD, Lutz M, Belperio JA, Keane MP, Strieter RM. The stromal derived factor-1/CXCL12-CXC chemokine receptor 4 biological axis in non-small cell lung cancer metastases. *Am J Respir Crit Care Med* 2003;167:1676-1686
49. Speetjens FM, Liefers GJ, Korbee CJ, Mesker WE, van de Velde CJ, van Vlierberghe RL, et al. Nuclear localization of CXCR4 determines prognosis for colorectal cancer patients. *Cancer Microenviron* 2009;2:1-7
50. Terasaki M, Sugita Y, Arakawa F, Okada Y, Ohshima K, Shigemori M. CXCL12/CXCR4 signaling in malignant brain tumors: A potential pharmacological therapeutic target. *Brain Tumor Pathol* 2011;28:89-97
51. Muller A, Homey B, Soto H, Ge N, Catron D, Buchanan ME, et al. Involvement of chemokine receptors in breast cancer metastasis. *Nature* 2001;410:50-56
52. Zlotnik A, Burkhardt AM, Homey B. Homeostatic chemokine receptors and organ-specific metastasis. *Nat Rev Immunol* 2011;11:597-606
53. Guo F, Wang Y, Liu J, Mok SC, Xue F, Zhang W. CXCL12/CXCR4: a symbiotic bridge linking cancer cells and their stromal neighbors in oncogenic communication networks. *Oncogene* 2016;35:816-826
54. Scala S. Molecular pathways: targeting the CXCR4-CXCL12 axis--untapped potential in the tumor microenvironment. *Clin Cancer Res* 2015;21:4278-4285
55. Bagri A, Gurney T, He X, Zou YR, Littman DR, Tessier-Lavigne M, et al. The chemokine SDF1 regulates migration of dentate granule cells. *Development* 2002;129:4249-4260
56. Kucia M, Reza R, Miekus K, Wanzeck J, Wojakowski W, Janowska-Wieczorek A, et al. Trafficking of normal stem cells and metastasis of cancer stem cells involve similar mechanisms: pivotal role of the SDF-1-CXCR4 axis. *Stem Cells* 2005;23:879-894
57. Teicher BA, Fricker SP. CXCL12 (SDF-1)/CXCR4 pathway in cancer. *Clin Cancer Res* 2010;16:2927-2931
58. Chatterjee S, Behnam Azad B, Nimmagadda S. The intricate role of CXCR4 in cancer. *Adv Cancer Res* 2014;124:31-82
59. Sun Y, Cheng Z, Ma L, Pei G. Beta-arrestin2 is critically involved in CXCR4-mediated chemotaxis, and this is mediated by its enhancement of p38 MAPK activation. *J Biol Chem* 2002;277:49212-49219
60. Liebick M, Henze S, Vogt V, Oppermann M. Functional consequences of chemically-induced  $\beta$ -arrestin binding to chemokine receptors CXCR4 and CCR5 in the absence of ligand stimulation. *Cell Signal* 2017;38:201-211
61. Wang Y, Wang Z, Jia F, Xu Q, Shu Z, Deng J, et al. CXCR4-guided liposomes regulating hypoxic and immunosuppressive microenvironment for sorafenib-resistant tumor treatment. *Bioact Mater* 2022;17:147-161
62. Xiao Y, Chen J, Zhou H, Zeng X, Ruan Z, Pu Z, et al. Combining p53 mRNA nanotherapy with immune checkpoint blockade reprograms the immune microenvironment for effective cancer therapy. *Nat Commun* 2022;13:758
63. Choueiri TK, Atkins MB, Rose TL, Alter RS, Ju Y, Niland K, et al. A phase 1b trial of the CXCR4 inhibitor mavorixafor and nivolumab in advanced renal cell carcinoma patients with no prior response to nivolumab monotherapy. *Invest New Drugs* 2021;39:1019-1027
64. Niu J, Huang Y, Zhang L. CXCR4 silencing inhibits invasion and migration of human laryngeal cancer Hep-2 cells. *Int J Clin Exp Pathol* 2015;8:6255-6261
65. Wester HJ, Keller U, Schottelius M, Beer A, Philipp-Abbrederis K, Hoffmann F, et al. Disclosing the CXCR4 expression in lymphoproliferative diseases by targeted molecular imaging. *Theranostics* 2015;5:618-630
66. Ahn JY, Seo K, Weinberg OK, Arber DA. The prognostic value of CXCR4 in acute myeloid leukemia. *Appl Immunohistochem Mol Morphol* 2013;21:79-84
67. Spoo AC, Lübbert M, Wierda WG, Burger JA. CXCR4 is a prognostic marker in acute myelogenous leukemia. *Blood* 2007;109:786-791
68. Hiller DJ, Meschonat C, Kim R, Li BD, Chu QD. Chemokine receptor CXCR4 level in primary tumors independently predicts outcome for patients with locally advanced breast cancer. *Surgery* 2011;150:459-465
69. Zucca E, Copie-Bergman C, Ricardi U, Thieblemont C, Raderer M, Ladetto M. Gastric marginal zone lymphoma of MALT type: ESMO Clinical Practice Guidelines for diagnosis, treatment and follow-up. *Ann Oncol* 2013;24 Suppl 6:vi144-vi148
70. Haug AR, Leisser A, Wadsak W, Mitterhauser M, Pfaff S, Kropf S, et al. Prospective non-invasive evaluation of CXCR4 expression for the diagnosis of MALT lymphoma using [(68)Ga]Ga-pentixafor-PET/MRI. *Theranostics* 2019;9:3653-3658
71. Mayerhoefer ME, Raderer M, Lamm W, Pichler V, Pfaff S, Weber M, et al. CXCR4 PET imaging of mantle cell lymphoma using [(68)Ga]Pentixafor: comparison with [(18)F]FDG-PET. *Theranostics* 2021;11:567-578
72. Fonseca R, Hayman S. Waldenström macroglobulinaemia. *Br J Haematol* 2007;138:700-720
73. Duell J, Krummenast F, Schirbel A, Klassen P, Samnick S, Rauert-Wunderlich H, et al. Improved primary staging of marginal-zone lymphoma by addition of CXCR4-directed PET/CT. *J Nucl Med* 2021;62:1415-1421
74. Pan Q, Cao X, Luo Y, Li J, Feng J, Li F. Chemokine receptor-4 targeted PET/CT with (68)Ga-pentixafor in assessment of newly diagnosed multiple myeloma: comparison to (18)F-FDG PET/CT. *Eur J Nucl Med Mol Imaging* 2020;47:537-546
75. Walker RC, Brown TL, Jones-Jackson LB, De Blanche L, Bartel T. Imaging of multiple myeloma and related plasma cell dyscrasias. *J Nucl Med* 2012;53:1091-1101
76. Lapa C, Schreder M, Schirbel A, Samnick S, Kortüm KM, Herrmann K, et al. [(68)Ga]Pentixafor-PET/CT for imaging of chemokine receptor CXCR4 expression in multiple myeloma - comparison to [(18)F]FDG and laboratory values. *Theranostics* 2017;7:205-212
77. Mayerhoefer ME, Jaeger U, Staber P, Raderer M, Wadsak W, Pfaff S, et al. [(68)Ga]Ga-pentixafor PET/MRI for CXCR4

- imaging of chronic lymphocytic leukemia: preliminary results. *Invest Radiol* 2018;53:403-408
78. Spivak JL. Myeloproliferative neoplasms. *N Engl J Med* 2017;376:2168-2181
  79. Kraus S, Dierks A, Rasche L, Kertels O, Kircher M, Schirbel A, et al. (68)Ga-pentixafor PET/CT for detection of chemokine receptor CXCR4 expression in myeloproliferative neoplasms. *J Nucl Med* 2022;63:96-99
  80. Yang H, Chen YX. Improvement analysis of article quality in World Journal of Gastroenterology during 2008-2012. *World J Gastroenterol* 2013;19:7830-7835
  81. Kaifi JT, Yekebas EF, Schurr P, Obonyo D, Wachowiak R, Busch P, et al. Tumor-cell homing to lymph nodes and bone marrow and CXCR4 expression in esophageal cancer. *J Natl Cancer Inst* 2005;97:1840-1847
  82. Wang X, Cao Y, Zhang S, Chen Z, Fan L, Shen X, et al. Stem cell autocrine CXCL12/CXCR4 stimulates invasion and metastasis of esophageal cancer. *Oncotarget* 2017;8:36149-36160
  83. Zhang M, Zhang L, Cui M, Ye W, Zhang P, Zhou S, et al. miR-302b inhibits cancer-related inflammation by targeting ERBB4, IRF2 and CXCR4 in esophageal cancer. *Oncotarget* 2017;8:49053-49063
  84. Linde P, Baues C, Wegen S, Trommer M, Quaas A, Rosenbrock J, et al. Pentixafor PET/CT for imaging of chemokine receptor 4 expression in esophageal cancer - a first clinical approach. *Cancer Imaging* 2021;21:22
  85. Grueneisen J, Nagarajah J, Buchbender C, Hoffmann O, Schaarschmidt BM, Poeppel T, et al. Positron emission tomography/magnetic resonance imaging for local tumor staging in patients with primary breast cancer: a comparison with positron emission Tomography/Computed tomography and magnetic resonance imaging. *Invest Radiol* 2015;50:505-513
  86. Garcia-Velloso MJ, Ribelles MJ, Rodriguez M, Fernandez-Montero A, Sancho L, Prieto E, et al. MRI fused with prone FDG PET/CT improves the primary tumour staging of patients with breast cancer. *Eur Radiol* 2017;27:3190-3198
  87. Liang X, Yu J, Wen B, Xie J, Cai Q, Yang Q. MRI and FDG-PET/CT based assessment of axillary lymph node metastasis in early breast cancer: a meta-analysis. *Clin Radiol* 2017;72:295-301
  88. Weiss ID, Jacobson O. Molecular imaging of chemokine receptor CXCR4. *Theranostics* 2013;3:76-84
  89. Philipp-Abbrederis K, Herrmann K, Knop S, Schottelius M, Eiber M, Lückerath K, et al. In vivo molecular imaging of chemokine receptor CXCR4 expression in patients with advanced multiple myeloma. *EMBO Mol Med* 2015;7:477-487
  90. George GP, Pisaneschi F, Stevens E, Nguyen QD, Åberg O, Spivey AC, et al. Scavenging strategy for specific activity improvement: application to a new CXCR4-specific cyclopentapeptide positron emission tomography tracer. *J Labelled Comp Radiopharm* 2013;56:679-685
  91. Smith MC, Luker KE, Garbow JR, Prior JL, Jackson E, Pivnicka-Worms D, et al. CXCR4 regulates growth of both primary and metastatic breast cancer. *Cancer Res* 2004;64:8604-8612
  92. Vag T, Steiger K, Rossmann A, Keller U, Noske A, Herhaus P, et al. PET imaging of chemokine receptor CXCR4 in patients with primary and recurrent breast carcinoma. *EJNMMI Res* 2018;8:90
  93. Nagarsheth N, Wicha MS, Zou W. Chemokines in the cancer microenvironment and their relevance in cancer immunotherapy. *Nat Rev Immunol* 2017;17:559-572
  94. Fu P, Tian L, Cao X, Li L, Xu P, Zhao C. Imaging CXCR4 expression with (99m)Tc-radiolabeled small-interference RNA in experimental human breast cancer xenografts. *Mol Imaging Biol* 2016;18:353-359
  95. Zhao Y, Detering L, Sultan D, Cooper ML, You M, Cho S, et al. Gold nanoclusters doped with (64)Cu for CXCR4 positron emission tomography imaging of breast cancer and metastasis. *ACS Nano* 2016;10:5959-5970
  96. Li H, Zhang X, Wu HY, Sun L, Ma Y, Xu J, et al. (64)Cu-labeled ubiquitin for PET imaging of CXCR4 expression in mouse breast tumor. *ACS Omega* 2019;4:12432-12437
  97. Demoin DW, Shindo M, Zhang H, Edwards KJ, Serganova I, Pillarsetty NV, et al. Synthesis and evaluation of an (18)F-labeled pyrimidine-pyridine amine for targeting CXCR4 receptors in gliomas. *Nucl Med Biol* 2016;43:606-611
  98. Chiang GC, Kovanlikaya I, Choi C, Ramakrishna R, Magge R, Shungu DC. Magnetic resonance spectroscopy, positron emission tomography and radiogenomics-relevance to glioma. *Front Neurol* 2018;9:33
  99. Galldiks N, Lohmann P, Albert NL, Tonn JC, Langen KJ. Current status of PET imaging in neuro-oncology. *Neurooncol Adv* 2019;1:vdz010
  100. Hutterer M, Nowosielski M, Putzer D, Jansen NL, Seiz M, Schocke M, et al. [(18)F]-fluoro-ethyl-L-tyrosine PET: a valuable diagnostic tool in neuro-oncology, but not all that glitters is glioma. *Neuro Oncol* 2013;15:341-351
  101. Hartimath SV, van Waarde A, Dierckx RA, de Vries EF. Evaluation of N-[(11)C]Methyl-AMD3465 as a PET tracer for imaging of CXCR4 receptor expression in a C6 glioma tumor model. *Mol Pharm* 2014;11:3810-3817
  102. Zhang H, Maeda M, Shindo M, Ko M, Mane M, Grommes C, et al. Imaging CXCR4 expression with iodinated and brominated cyclam derivatives. *Mol Imaging Biol* 2020;22:1184-1196
  103. Jacobs SM, Wesseling P, de Keizer B, Tolboom N, Ververs F, Krijger GC, et al. CXCR4 expression in glioblastoma tissue and the potential for PET imaging and treatment with [(68)Ga]Ga-pentixafor /[(177)Lu]Lu-pentixather. *Eur J Nucl Med Mol Imaging* 2022;49:481-491
  104. Shiels MS, Pfeiffer RM, Besson C, Clarke CA, Morton LM, Nogueira L, et al. Trends in primary central nervous system lymphoma incidence and survival in the U.S. *Br J Haematol* 2016;174:417-424
  105. Mendez JS, Ostrom QT, Gittleman H, Kruchko C, DeAngelis LM, Barnholtz-Sloan JS, et al. The elderly left behind-changes in survival trends of primary central nervous system lymphoma over the past 4 decades. *Neuro Oncol*



- 2018;20:687-694
106. Villano JL, Koshy M, Shaikh H, Dolecek TA, McCarthy BJ. Age, gender, and racial differences in incidence and survival in primary CNS lymphoma. *Br J Cancer* 2011;105:1414-1418
  107. Herhaus P, Lipkova J, Lammer F, Yakushev I, Vag T, Slotta-Huspenina J, et al. CXCR4-targeted PET imaging of central nervous system B-Cell lymphoma. *J Nucl Med* 2020;61:1765-1771
  108. Boehme V, Zeynalova S, Kloess M, Loeffler M, Kaiser U, Pfreundschuh M, et al. Incidence and risk factors of central nervous system recurrence in aggressive lymphoma--a survey of 1693 patients treated in protocols of the German High-Grade Non-Hodgkin's Lymphoma Study Group (DSHNHL). *Ann Oncol* 2007;18:149-157
  109. Deckert M, Engert A, Brück W, Ferreri AJ, Finke J, Illerhaus G, et al. Modern concepts in the biology, diagnosis, differential diagnosis and treatment of primary central nervous system lymphoma. *Leukemia* 2011;25:1797-1807
  110. Korfel A, Schlegel U. Diagnosis and treatment of primary CNS lymphoma. *Nat Rev Neurol* 2013;9:317-327
  111. Doolittle ND, Abrey LE, Shenkier TN, Tali S, Bromberg JE, Neuwelt EA, et al. Brain parenchyma involvement as isolated central nervous system relapse of systemic non-Hodgkin lymphoma: an International Primary CNS Lymphoma Collaborative Group report. *Blood* 2008;111:1085-1093
  112. Dreyling M, Campo E, Hermine O, Jerkeman M, Le Gouill S, Rule S, et al. Newly diagnosed and relapsed mantle cell lymphoma: ESMO clinical practice guidelines for diagnosis, treatment and follow-up. *Ann Oncol* 2017;28(suppl 4):iv62-iv71
  113. Toh CH, Castillo M, Wong AM, Wei KC, Wong HF, Ng SH, et al. Primary cerebral lymphoma and glioblastoma multiforme: differences in diffusion characteristics evaluated with diffusion tensor imaging. *AJNR Am J Neuroradiol* 2008;29:471-475
  114. Abrey LE, Batchelor TT, Ferreri AJ, Gospodarowicz M, Pulczynski EJ, Zucca E, et al. Report of an international workshop to standardize baseline evaluation and response criteria for primary CNS lymphoma. *J Clin Oncol* 2005;23:5034-5043
  115. Nabavizadeh SA, Vossough A, Hajmomenian M, Assadsangabi R, Mohan S. Neuroimaging in central nervous system lymphoma. *Hematol Oncol Clin North Am* 2016;30:799-821
  116. Baraniskin A, Deckert M, Schulte-Altdorneburg G, Schlegel U, Schroers R. Current strategies in the diagnosis of diffuse large B-cell lymphoma of the central nervous system. *Br J Haematol* 2012;156:421-432
  117. Starzer AM, Berghoff AS, Traub-Weidinger T, Haug AR, Widhalm G, Hacker M, et al. Assessment of central nervous system lymphoma based on CXCR4 expression in vivo using (68)Ga-pentixafor PET/MRI. *Clin Nucl Med* 2021;46:16-20
  118. Stemmer-Rachamimov AO, Louis DN, Nielsen GP, Antonescu CR, Borowsky AD, Bronson RT, et al. Comparative pathology of nerve sheath tumors in mouse models and humans. *Cancer Res* 2004;64:3718-3724
  119. Breun M, Monoranu CM, Kessler AF, Matthies C, Löhr M, Hagemann C, et al. [(68)Ga]-pentixafor PET/CT for CXCR4-mediated imaging of vestibular schwannomas. *Front Oncol* 2019;9:503
  120. Lapa C, Herrmann K, Schirbel A, Hänscheid H, Lückertath K, Schottelius M, et al. CXCR4-directed endoradiotherapy induces high response rates in extramedullary relapsed multiple myeloma. *Theranostics* 2017;7:1589-1597